

## Phase Space Tweezers for Tailoring Cavity Fields by Quantum Zeno Dynamics

J. M. Raimond,<sup>1</sup> C. Sayrin,<sup>1</sup> S. Gleyzes,<sup>1</sup> I. Dotsenko,<sup>1</sup> M. Brune,<sup>1</sup> S. Haroche,<sup>1,2</sup> P. Facchi,<sup>3,4</sup> and S. Pascazio<sup>5,4</sup>

<sup>1</sup>Laboratoire Kastler Brossel, CNRS, ENS, UPMC-Paris 6, 24 rue Lhomond, 75231 Paris, France

<sup>2</sup>Collège de France, 11 place Marcelin Berthelot, 75231 Paris, France

<sup>3</sup>Dipartimento di Matematica and MECENAS, Università di Bari, I-70125 Bari, Italy

<sup>4</sup>INFN, Sezione di Bari, I-70126 Bari, Italy

<sup>5</sup>Dipartimento di Fisica and MECENAS, Università di Bari, I-70126 Bari, Italy

(Received 27 July 2010; published 16 November 2010)

We discuss an implementation of quantum Zeno dynamics in a cavity quantum electrodynamics experiment. By performing repeated unitary operations on atoms coupled to the field, we restrict the field evolution in chosen subspaces of the total Hilbert space. This procedure leads to promising methods for tailoring nonclassical states. We propose to realize “tweezers” picking a coherent field at a point in phase space and moving it towards an arbitrary final position without affecting other nonoverlapping coherent components. These effects could be observed with a state-of-the-art apparatus.

DOI: 10.1103/PhysRevLett.105.213601

PACS numbers: 42.50.Pq, 03.65.Xp, 42.50.Dv

In the quantum Zeno effect (QZE) [1], repeated projective measurements block the evolution of a system in a non-degenerate eigenstate of the measured observable. It has been observed on two-level systems [2] and on a harmonic oscillator in a cavity quantum electrodynamics (CQED) experiment [3]. A quantum Zeno dynamics (QZD) [4] takes place when the system is not confined to a single state, but rather evolves under the action of its free Hamiltonian  $H$  in a multidimensional subspace of its Hilbert space. This can be achieved either by repeated measurements of an observable with degenerate eigenvalues, or by repeated actions of a unitary kick  $U_K$  with multidimensional invariant subspaces, the two procedures being physically equivalent [5]. We focus here on the latter case, related to the so-called “bang-bang” control [6] and NMR manipulation techniques [7].

The system evolution is stroboscopic, alternating small free evolution steps described by  $U(\delta t) = \exp(-iH\delta t/\hbar)$  with  $U_K$  kicks. The succession of  $N$  steps (fixed duration  $t = N\delta t$ ) corresponds to the unitary  $U_Z(N) = [U_K U(t/N)]^N$ . It is, in the  $N \rightarrow \infty$  limit, the evolution under an effective Hamiltonian  $H_Z = \sum_{\mu} P_{\mu} H P_{\mu}$  where the  $P_{\mu}$ 's are the projectors on the invariant subspaces of  $U_K$  [4]. By choosing properly  $U_K$  (or equivalently the repeatedly measured observable), one can tailor the system evolution, leading to decoherence control [5], state purification [8] and quantum-gate implementation [9]. QZD can also inhibit entanglement between subsystems, making a quantum evolution semiclassical [10].

In this Letter, we propose a CQED implementation of the bang-bang QZD control. We exploit the nonlinearity of the atom-cavity system [11] to implement a photon-number-selective  $U_K$ . The field dynamics in its Hilbert space  $\mathcal{H}$  is confined in two orthogonal subspaces  $\mathcal{H}_{<s}$  and  $\mathcal{H}_{>s}$ , corresponding to photon numbers smaller or larger than a preset value  $s$ . This leads to novel methods of

nonclassical field states preparation and tailoring. We propose a “phase space tweezer” picking selectively a coherent state component of a quantum superposition and moving it at will in phase space independently from the other components.

Our proposal could be implemented in a microwave CQED experiment with circular Rydberg atoms and a superconducting millimeter-wave cavity [11]. The cavity  $C$  [Fig. 1(a)] is crossed by a slow beam of Rubidium ground state atoms, in an “atomic fountain” arrangement. Close to their turning point, atoms are nearly at rest. One of them is promoted to the circular level  $h$  (principal quantum number 49) using static and radio-frequency electric

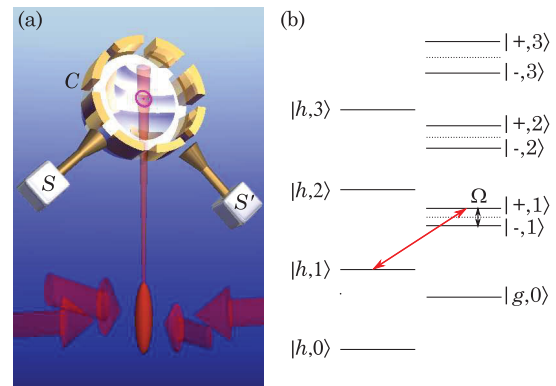


FIG. 1 (color). (a) Proposed experimental scheme. A slow atomic beam extracted from a 2D-magneto-optical trap (bottom) forms an atomic fountain with atoms nearly at rest in the center of the high-quality microwave Fabry-Perot cavity  $C$  (only one mirror shown). Sources  $S$  and  $S'$  address, respectively, the dressed atomic levels and the cavity mode. Electrodes around the cavity mirrors generate the electric fields preparing the circular state shown in the center. (b) Scheme of the dressed atomic levels. The arrow indicates the photon-number selective transition addressed by  $S$  for  $s = 1$ .

fields. This operation does not change the state of  $C$ , tuned on resonance with the 51.1 GHz transition between  $g$  and  $e$  (50 and 51 circular states). The analysis that follows pertains to the dynamics of this single atom and the cavity.

The source  $S$  drives the  $h \rightarrow g$  transition near 54.3 GHz. It does not couple directly to the off-resonant cavity. It realizes  $U_K$  by probing the eigenstates of the atom-cavity system [Fig. 1(b)]. The energies of the  $|h, n\rangle$  states (atom in  $h$  with  $n$  photons) do not depend on the atom-cavity coupling, since  $C$  is far off-resonance from the  $h \rightarrow g$  transition. The source  $S$  couples  $|h, n\rangle$  to the dressed states  $|\pm, n\rangle = (|e, n-1\rangle \pm |g, n\rangle)/\sqrt{2}$ , which are superpositions of the degenerate uncoupled states  $|e, n-1\rangle, |g, n\rangle$ . The splitting between dressed states is  $\Omega\sqrt{n}$  where  $\Omega$  is the vacuum Rabi frequency. Hence, the  $|h, n\rangle \rightarrow |+, n\rangle$  transition frequency depends upon  $n$ . We tune  $S$  to perform on the  $|h, s\rangle \rightarrow |+, s\rangle$  transition a  $2\pi$  Rabi pulse whose amplitude is weak enough (and its duration correspondingly long enough) not to appreciably affect  $|h, n\rangle$  with  $n \neq s$ . It results in the transformation  $|h, n\rangle \rightarrow (-1)^{\delta_{ns}}|h, n\rangle$ . The atom always ends up in  $h$  while the field experiences  $U_K = U_s$  with  $U_s = \mathbb{1} - 2|s\rangle\langle s|$ . Such a photon-number dependent Rabi pulse [12] was used with  $s = 1$  for a single-photon quantum-nondemolition detection [13] and for a controlled-NOT (CNOT) gate in CQED [14].

The free cavity dynamics is produced by the source  $S'$ , resonantly coupled with  $C$  and acting during time intervals  $\delta t$  between two  $U_s$  operations. Being not resonant with the atom in  $h$ ,  $S'$  leaves it unaffected. The free evolution is described by the Hamiltonian  $H = -i(\mathcal{E}^*a - \mathcal{E}a^\dagger)$ , where  $\mathcal{E}$  is the source amplitude and  $a$  ( $a^\dagger$ ) the photon annihilation (creation) operator. We use an interaction representation eliminating the field phase rotation at cavity frequency. The unitary  $U(\delta t)$  is the displacement  $D(\beta) = \exp(\beta a^\dagger - \beta^* a)$ , with  $\beta = \mathcal{E}\delta t/\hbar \ll 1$ . After  $p$  repetitions of  $U_s U(\delta t)$ , the cavity state can be reconstructed [15].

The eigenvalues of  $U_s$  are  $-1$  and  $+1$ . The former corresponds to the one-dimension eigenspace  $\mathcal{H}_{<s}$ , generated by

$|s\rangle$  (projector  $P_s$ ). The latter is associated to the direct sum of  $\mathcal{H}_{<s}$  (projector  $P_{<s}$ ), generated by the Fock states  $|0\rangle, \dots, |s-1\rangle$ , and  $\mathcal{H}_{>s}$  (projector  $P_{>s}$ ) generated by Fock states above  $|s\rangle$ . The projectors  $P_\mu$  ( $\mu = +, -$ ) are thus  $P_- = P_s$  and  $P_+ = P_{<s} + P_{>s}$ .

Since  $H$  is a linear combination of  $a$  and  $a^\dagger$ ,  $H_Z$  reduces to  $P_{<s}HP_{<s} + P_{>s}HP_{>s}$ . Under the QZD, field states restricted to  $\mathcal{H}_{<s}$  and  $\mathcal{H}_{>s}$  remain confined in these subspaces,  $|s\rangle$  realizing a hard “wall” between them. This wall induces remarkable features in the evolution. If we start from the vacuum in  $C$  with  $s = 1$ , the system remains inside  $\mathcal{H}_{<1}$ , i.e., in  $|0\rangle$ . We recover the QZE [3].

We have simulated this QZD procedure [16]. Figure 2(a) presents 10 snapshots of the field Wigner function,  $W(\xi)$ , separated by intervals of 5 steps, for  $s = 6$  and  $\beta = 0.1$ . The field starts from  $|0\rangle \in \mathcal{H}_{<6}$ . Its amplitude first increases along the real axis (free dynamics). Between 15 and 20 steps, the amplitude reaches  $\approx 2$  and QZD comes into play. The coherent state “collides” on the  $U_s$ -induced “wall,” materialized in phase space as an “exclusion circle” (EC) of radius  $\sqrt{6}$  (dashed line in Fig. 2). The field amplitude stops growing and undergoes a progressive  $\pi$  phase shift between steps 20 and 30. At step 25, the field is in a “cat state,” quantum superposition of two components with opposite phases. The fringing feature inside the EC is the signature of the quantum coherence of this superposition. This cat contains only odd photon numbers (probabilities for 5, 3, and 1 photons are 0.63, 0.31, and 0.03). At step 35, the field state is nearly coherent with an amplitude close to  $-2$ . It then resumes its motion from left to right along the real axis, going through  $|0\rangle$  again (around step 45) and heading towards its next “collision” with the EC.

Figure 3 presents the long-term evolution of the field energy. During the first few hundred steps, the oscillations reveal the quasiperiodic motion of the field inside the EC. State distortions, however, accumulate and damp the oscillations, whose contrast nearly vanishes after 800 steps. Since there is only a finite set of frequencies in  $P_{<6}HP_{<6}$ ,

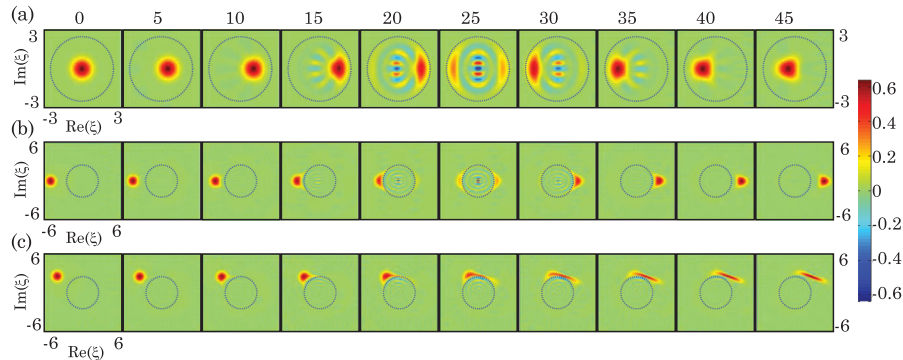


FIG. 2 (color). (a) QZD dynamics in  $\mathcal{H}_{<6}$ . Ten snapshots of the field Wigner function  $W(\xi)$  obtained after a number of steps indicated above each frame. The cavity is initially in its vacuum state,  $s = 6$  and  $\beta = 0.1$ . The EC is plotted as a blue dashed line. (b) QZD dynamics in  $\mathcal{H}_{>6}$ . Same as (a) with an initial  $\alpha = -5$  amplitude. (c) Same as (b), with an initial amplitude  $\alpha = -4 + i\sqrt{6}$ . In (b) and (c) the successive frames correspond to the same step numbers as in (a).

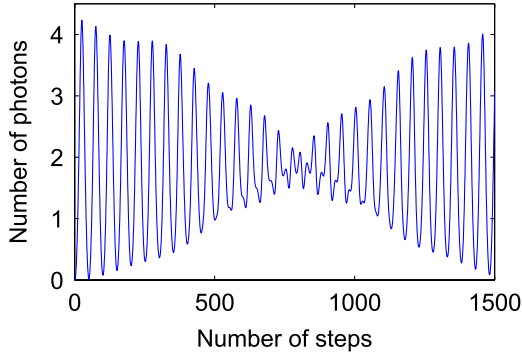


FIG. 3 (color online). Energy of the field as a function of the number of steps for a QZD dynamics inside  $\mathcal{H}_{<6}$ . Conditions are the same as for Fig. 2(a), which presents snapshots of the first oscillation.

we observe at longer times a quantum revival [11]. The energy oscillations resume and the field comes back to an oscillating coherent state periodically colliding with the EC as described above.

Figure 2(b) illustrates QZD in  $\mathcal{H}_{>s}$  with snapshots of the field Wigner function for  $s = 6$  and an initial coherent state  $|\alpha = -5\rangle$ . The field collides on the EC after 20 steps. It undergoes a QZD-induced  $\pi$  phase shift being, after 25 steps, in a cat state. After 30 steps, the state is again nearly coherent with a positive amplitude. It resumes its motion along the real axis. After 45 steps, its amplitude is slightly larger than 4.5. It would be  $-0.5$  in the case of free dynamics. The QZD-induced phase inversion accelerates the “propagation” in phase space. This opens interesting possibilities when the initial amplitude is such that the field state collides tangentially on the EC. The parts of the Wigner function that come closest to the EC propagate faster than others. The state is distorted and ends up strongly squeezed [Fig. 2(c)].

QZD can be generalized to ECs centered at an arbitrary point  $\gamma$  in phase space by changing the kick operator  $U_K$  from  $U_s$  to  $U_s(\gamma) = D(\gamma)U_sD(-\gamma)$  (these displacements  $\gamma$  being also performed by  $S'$ ). After  $p$  steps, the global evolution operator is  $U_Z(s, \gamma, p) = [U_s(\gamma)D(\beta)]^p$  which can be expressed, using displacement operator commutation relations, as  $U_Z(s, \gamma, p) = D(\gamma)U_Z(s, 0, p)D(-\gamma)\exp[2ip\text{Im}(\beta\gamma^*)]$ . Up to a topological phase, the state after  $p$  steps is equivalently obtained by first displacing the field by  $-\gamma$ , performing  $p$  QZD steps in an EC centered at origin and finally displacing back the field by  $\gamma$ .

This leads to the concept of phase space tweezer. Applying this procedure with  $s = 1$  to an initial cat state  $|\gamma\rangle + |\alpha\rangle$  ( $\langle\gamma|\alpha\rangle \approx 0$ ), we can selectively block the evolution of  $|\gamma\rangle$  while leaving the other component free to evolve. After  $N$  steps, we get the “stretched” cat  $|\gamma\rangle + D(N\beta)|\alpha\rangle = |\gamma\rangle + \exp[iN\text{Im}(\beta\alpha^*)]|\alpha + N\beta\rangle$ .

In an interesting variant, the position  $\gamma_p$  of the tweezer is changed by a small amount at each step  $p$  ( $|\gamma_{p+1} - \gamma_p| \ll 1$ ), while  $\beta$  is set to zero (no free evolution). The sequence of

$\{\gamma_p\}$  defines a trajectory  $\mathcal{T}$  in phase space followed by the center of the EC. A coherent state with the initial amplitude  $\alpha_i = \gamma_1$  follows adiabatically this trajectory and becomes, after the  $p$ th step, a coherent state with amplitude  $\alpha_p = \gamma_p$ . We realize in this way a tweezer which moves one selected coherent state, while not affecting the evolution of all the coherent states whose amplitude remains away from  $\mathcal{T}$ .

A combination of tweezers can move all the components of a superposition of nonoverlapping coherent states from arbitrary initial to final positions. An obvious method is to grasp them one by one, driving them from their initial to their final position (taking care to move them so that different components never overlap). The tweezers can also be used in parallel by applying incremental motions alternatively on each component.

Figure 4 illustrates this procedure for a two-component cat, initially  $|\alpha\rangle + |-\alpha\rangle$  with  $\alpha = 2$ . It is turned in 100 steps (50 on each component) into  $|\alpha'\rangle + |-\alpha'\rangle$  with  $\alpha' = 5i$ . Panels (a) and (b) present the initial and final Wigner functions. The final fidelity is 98.8% with respect to the expected cat. It remains greater than 68% if the operation is performed in 20 steps only, exhibiting the robustness of this adiabatic procedure, which is promising for experimental implementations.

The initial cat state can be generated in various ways using dispersive [17] or resonant [18] atoms. An adapted tweezer procedure also prepares from  $|0\rangle$  mesoscopic superpositions which are approximations of these cat states.

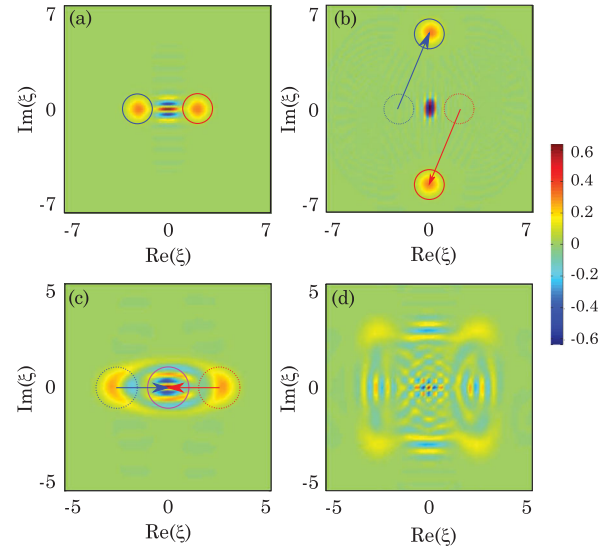


FIG. 4 (color). (a),(b) Initial and final Wigner functions  $W(\xi)$  for a phase space tweezer operation. The first step ECs are depicted as solid lines in (a) and dotted lines in (b), the final ECs as solid lines in (b). The arrows in (b) indicate the two EC centers trajectories. (c) Cat created by a vacuum state crush operation. Initial (dotted lines) and final (solid line) ECs are plotted, with arrows indicating the motion of their centers. (d) Four-component cat created by three successive crushing operations.

We “crush” the vacuum between two  $s = 1$  ECs whose centers, initially at  $\pm 2.5$ , move simultaneously towards each other in 200 steps, until they reach the origin (the wave function remaining outside both ECs). Figure 4(c) presents the final Wigner function. The state is a superposition of two well-separated components (average energy 6.4 photons). Its fidelity with respect to a  $|\alpha\rangle + |-\alpha\rangle$  cat with the same average energy is 42%. The final components can be crushed again and so on, leading to a superposition state with an arbitrary number of components. Figure 4(c) presents the Wigner function of a four-component cat obtained by crushing again each of the two components in Fig. 4(b) between ECs moving towards each other along the imaginary axis direction.

QZD is also obtained when the interrogation pulse has a Rabi angle  $\theta$  different from  $2\pi$ . The pulse performs then a unitary kick acting on the atom-cavity system, which mixes  $|h, s\rangle$  with  $|+, s\rangle$  and would create atom-field entanglement if  $C$  contained  $s$  photons. This unitary admits an invariant subspace, belonging to the eigenvalue  $+1$  spanned by the projection  $|h\rangle\langle h| \otimes (P_{<s} + P_{>s})$ , the same as for a  $2\pi$  pulse. Starting from an atom in  $|h\rangle$  and a field in  $\mathcal{H}_{<s}$  or  $\mathcal{H}_{>s}$ , we obtain a QZD leaving the atom in  $|h\rangle$  and the field in its initial subspace. Under perfect QZD, the cavity *never* contains  $s$  photons and the atom and field are *never* entangled by the interrogation pulse. Obviously, QZD is not achieved if  $\theta$  is very small, each kick operation being too close to  $\mathbb{1}$ . We have checked numerically that, for  $\theta \approx 1$ , we recover within a good approximation all the results described above.

Numerical simulations can take into account realistic experimental imperfections. We have simulated an experiment in construction [Fig. 1(a)], with a cavity damping time  $T_c = 0.13$  s and  $\Omega/2\pi = 50$  kHz [15]. We have taken into account the limited selectivity of the interrogation pulse, which must be at the same time much shorter than  $T_c$  and much longer than  $1/\Omega$ . We have optimized the interrogation pulse parameters for a tweezer operation leading, in 10 steps (2.3 ms total duration), from an  $|\alpha = -2\rangle + |\alpha = 2\rangle$  cat to  $|\alpha = -3\rangle + |\alpha = 3\rangle$ . The final fidelity with respect to the ideal cat is 70%.

Quantum Zeno dynamics applied to a field oscillator leads to novel methods for tailoring nonclassical fields and studying their decoherence [17]. Phase space tweezers could be used to prepare from the vacuum  $|0\rangle$  an arbitrary superposition of nonoverlapping coherent states  $\sum_i c_i |\gamma_i\rangle$ . The procedure, described elsewhere [19], uses a sequence of tweezing operations, each leading from  $|0\rangle$  to one of the  $|\gamma_i\rangle$ 's. At each step  $i$ , the tweezer atom is prepared in a superposition of  $h$  with an extra state  $f$  inactive in the tweezing process. This step transforms  $|0\rangle$  into a controlled

superposition of  $|0\rangle$  and  $|\gamma_i\rangle$ , leaving the  $|\gamma_j\rangle$ 's ( $j < i$ ) invariant.

Experimental demonstrations are within reach of a microwave CQED setup. They could also be implemented in circuit QED, where comparable  $\Omega T_c$  values are realized [20]. Manipulating at will the state of a quantum oscillator in its phase space provides a new insight into the physics of mesoscopic quantum superpositions and the exploration of the quantum to classical boundary.

We acknowledge support by the EU and ERC (AQUTE and DECLIC projects) and by the ANR (QUSCO-INCA).

- 
- [1] B. Misra and E. C. G. Sudarshan, *J. Math. Phys. (N.Y.)* **18**, 756 (1977); H. Nakazato *et al.*, *Int. J. Mod. Phys. B* **10**, 247 (1996); *Phys. Lett. A* **217**, 203 (1996); D. Home and M. A. B. Whitaker, *Ann. Phys. (N.Y.)* **258**, 237 (1997); K. Koshino and A. Shimizu, *Phys. Rep.* **412**, 191 (2005).
  - [2] W. M. Itano, D. J. Heinzen, J. J. Bollinger, and D. J. Wineland, *Phys. Rev. A* **41**, 2295 (1990); B. Nagels, L. J. F. Hermans and P. L. Chapovsky, *Phys. Rev. Lett.* **79**, 3097 (1997); P. G. Kwiat *et al.*, *Phys. Rev. Lett.* **83**, 4725 (1999); C. Balzer, R. Huesmann, W. Neuhauser, and P. Toschek, *Opt. Commun.* **180**, 115 (2000); E. W. Streed *et al.*, *Phys. Rev. Lett.* **97**, 260402 (2006); O. Hosten *et al.*, *Nature (London)* **439**, 949 (2006).
  - [3] J. Bernu *et al.*, *Phys. Rev. Lett.* **101**, 180402 (2008).
  - [4] P. Facchi and S. Pascazio, *Phys. Rev. Lett.* **89**, 080401 (2002); *J. Phys. A* **41**, 493001 (2008).
  - [5] P. Facchi, D. A. Lidar, and S. Pascazio, *Phys. Rev. A* **69**, 032314 (2004).
  - [6] L. Viola and S. Lloyd, *Phys. Rev. A* **58**, 2733 (1998).
  - [7] W. A. Anderson and F. A. Nelson, *J. Chem. Phys.* **39**, 183 (1963); R. R. Ernst, *J. Chem. Phys.* **45**, 3845 (1966); R. Freeman, S. P. Kempell, and M. H. Levitt, *J. Magn. Reson.* **35**, 447 (1979); M. H. Levitt, R. Freeman, and T. A. Frenkiel, *J. Magn. Reson.* **47**, 328 (1982).
  - [8] H. Nakazato, M. Unoki, and K. Yuasa, *Phys. Rev. A* **70**, 012303 (2004).
  - [9] X. Q. Shao *et al.*, *J. Opt. Soc. Am.* **26**, 2440 (2009).
  - [10] R. Rossi, K. M. Fonseca Romero and M. C. Nemes, *Phys. Lett. A* **374**, 158 (2009).
  - [11] S. Haroche and J. M. Raimond, *Exploring the Quantum* (Oxford University Press, Oxford, 2006).
  - [12] M. França Santos, E. Solano, and R. L. de Matos Filho, *Phys. Rev. Lett.* **87**, 093601 (2001).
  - [13] G. Noguez *et al.*, *Nature (London)* **400**, 239 (1999).
  - [14] A. Rauschenbeutel *et al.*, *Phys. Rev. Lett.* **83**, 5166 (1999).
  - [15] S. Deléglise *et al.*, *Nature (London)* **455**, 510 (2008).
  - [16] S. M. Tan, *J. Opt. B* **1**, 424 (1999).
  - [17] M. Brune *et al.*, *Phys. Rev. Lett.* **77**, 4887 (1996).
  - [18] A. Auffèves *et al.*, *Phys. Rev. Lett.* **91**, 230405 (2003).
  - [19] J. M. Raimond *et al.* (to be published).
  - [20] B. R. Johnson *et al.*, *Nature Phys.* **6**, 663 (2010).